



# EUROfusion

EUROFUSION WPPFC-PR(16) 14733

J Karhunen et al.

## **Measurement of $N^+$ flows in the HFS SOL of ASDEX Upgrade with different degrees of inner divertor detachment**

Preprint of Paper to be submitted for publication in  
22nd International Conference on Plasma Surface Interactions  
in Controlled Fusion Devices (22nd PSI)



This work has been carried out within the framework of the EUROfusion Consortium and has received funding from the Euratom research and training programme 2014-2018 under grant agreement No 633053. The views and opinions expressed herein do not necessarily reflect those of the European Commission.

This document is intended for publication in the open literature. It is made available on the clear understanding that it may not be further circulated and extracts or references may not be published prior to publication of the original when applicable, or without the consent of the Publications Officer, EUROfusion Programme Management Unit, Culham Science Centre, Abingdon, Oxon, OX14 3DB, UK or e-mail [Publications.Officer@euro-fusion.org](mailto:Publications.Officer@euro-fusion.org)

Enquiries about Copyright and reproduction should be addressed to the Publications Officer, EUROfusion Programme Management Unit, Culham Science Centre, Abingdon, Oxon, OX14 3DB, UK or e-mail [Publications.Officer@euro-fusion.org](mailto:Publications.Officer@euro-fusion.org)

The contents of this preprint and all other EUROfusion Preprints, Reports and Conference Papers are available to view online free at <http://www.euro-fusionscipub.org>. This site has full search facilities and e-mail alert options. In the JET specific papers the diagrams contained within the PDFs on this site are hyperlinked

# Measurement of $N^+$ flows in the high-field side scrape-off layer of ASDEX Upgrade with different degrees of inner divertor detachment

J. Karhunen<sup>a\*</sup>, M. Groth<sup>a</sup>, P. Heliste<sup>a</sup>, T. Pütterich<sup>b</sup>, E. Viezzer<sup>b</sup>, D. Carralero<sup>b</sup>, D. Coster<sup>b</sup>, L. Guimaraes<sup>c</sup>, A. Hakola<sup>d</sup>, V. Nikolaeva<sup>b,c,e</sup>, S. Potzel<sup>b</sup> and the ASDEX Upgrade Team

<sup>a</sup>*Aalto University, Department of Applied Physics, Espoo, Finland*

<sup>b</sup>*Max-Planck-Institut für Plasmaphysik, Garching, Germany*

<sup>c</sup>*Instituto de Plasmas e Fusão Nuclear, Instituto Superior Técnico, Lisboa, Portugal*

<sup>d</sup>*VTT Technical Research Centre of Finland Ltd., Espoo, Finland*

<sup>e</sup>*Physik-Department E28, Technische Universität München, Garching, Germany*

## Abstract

Toroidal and poloidal flows of injected  $N^+$  ions were measured in the high-field side (HFS) scrape-off layer (SOL) of ASDEX Upgrade by Doppler spectroscopy with different degrees of HFS divertor detachment. In high-recycling conditions, the results suggest reversed toroidal  $N^+$  flow in counter-current direction close to the separatrix, while the flow is co-current throughout the SOL in detached conditions. The measured poloidal  $N^+$  flows were directed away from the HFS divertor close to the separatrix for all density cases, suggesting possible dominance of the  $\mathbf{E}_r \times \mathbf{B}$  drift in this region. Divertor plasma oscillations, characterized by momentary peaking of the HFS target ion flux and decrease of the HFS SOL density observed slightly before the roll-over of the ion saturation current to the HFS target, lead to an increase in the  $N^+$  flow towards the HFS divertor. SOLPS and ERO simulations of the experiment predict entrainment below 50% between the velocities of  $N^+$  and  $D^+$  ions, suggesting that  $N^+$  ions are quantitatively a limited proxy for measuring  $D^+$  flows. ERO simulations show significantly higher entrainment for higher ionization states, e.g.,  $N^{2+}$  and  $N^{3+}$ .

*Keywords:* Impurity migration, Doppler spectroscopy, SOL flow, Divertor detachment

\* *Corresponding author email:* [juuso.karhunen@aalto.fi](mailto:juuso.karhunen@aalto.fi)

## 1. Introduction

Identifying plasma flows in the scrape-off layer (SOL) is essential for understanding material migration in the tokamak edge plasma. While SOL flows on the low-field side (LFS) of the plasma have been widely studied in several tokamaks [1], only few measurements exist on the high-field side (HFS). As the flow on the HFS has been observed to be stronger than on the LFS [2,3], and since it is considered responsible for material migration from the HFS wall to the HFS divertor, HFS SOL is a specific region of interest for new experiments. Direct Langmuir probe measurements of the  $D^+$  flow have been performed in the HFS midplane region of Alcator C-Mod [2,4] and in the HFS divertor region of ASDEX Upgrade [5,6] and JT-60U [3], whereas indirect measurements by spectroscopy and camera imaging have been carried out in the HFS midplane region of ASDEX Upgrade and Alcator C-Mod with the help of methane and nitrogen injections [7—9].

In this contribution, HFS SOL flows of  $N^+$  ions, originated from an  $N_2$  injection, have been measured by Doppler spectroscopy in the midplane region of ASDEX Upgrade in a similar fashion as in [7,8]. The flows were measured during L-mode discharges with varying degree of HFS divertor detachment to provide insight on the differences in flows under detached and high-recycling plasma conditions. The entrainment of the  $N^+$  ions with the background  $D^+$  plasma was studied by modelling the experiment with the SOLPS [10] and ERO [11] codes to assess, whether the  $N^+$  ions can be used as a representative proxy for measuring the  $D^+$  flows.

## 2. Experiment

The flow measurements were performed in six L-mode discharges (AUG shot numbers 32125, 32130—33, 32136) with plasma current, electron cyclotron resonance heating and ohmic heating of  $I_p=0.8$  MA,  $P_{ECRH}=0.3$  MW and  $P_{Ohm}=0.4—0.6$  MW, respectively. The discharges had a lower-single-null configuration with low triangularity and a gap of approximately 10 cm between the separatrix and the inner wall. To reach different degrees of HFS divertor detachment, the core electron density ( $n_e$ ) was varied between the discharges. One discharge (32125) was a density ramp within a range of  $n_e=2.0—6.0 \times 10^{19} \text{ m}^{-3}$ , providing information on the evolution of the HFS divertor conditions with increasing density. Based on this discharge, different representative densities were selected for the remaining discharges, as presented in figure 1. The densities correspond to approximately 20—60% of the Greenwald density limit. The evolution of detachment was monitored by the target Langmuir probes [12], while the HFS SOL density was measured by Stark broadening of the Balmer lines in the divertor volume [13] and by reflectometry in the HFS midplane region [14].

$N_2$  was injected into the plasma through a single valve in the inner heat shield 13 cm above the HFS midplane. Line-integrated emission of the injected nitrogen was recorded at different radial locations by seven toroidal and poloidal spectroscopic lines-of-sight (LOS) of the edge charge exchange recombination spectroscopy (CXRS) system [15,16]. To enhance the radial resolution of the measurements, the plasma was swept radially by roughly 1 cm during the discharges. The contribution of recycled nitrogen in the LFS SOL close to the ends of the LOS was eliminated by subtraction of the background emission measured by separate toroidal and poloidal LOS not directly observing the injection. The spectroscopic set-up is illustrated in figure 1 of [8].

## 3. HFS divertor conditions

The evolution of the integrated total ion flux and strike-point electron temperature at the HFS target, given by the target Langmuir probes, is presented in figures 2a—b as a function of the

core electron density. The target ion flux first increases with core density, until it rolls over at  $n_e=4.0\times 10^{19} \text{ m}^{-3}$  and starts to decrease, while the target temperature is always below 5 eV. This suggests that the vertical section of the HFS target plate ranged from high-recycling to detached conditions during the experiment.

The divertor spectroscopy data, presented in figure 2c, shows spreading of a high-density front with  $n_{e,\text{SOL}}=2\text{--}5\times n_{e,\text{core}}$  upwards from the HFS strike-point region with increasing core density, agreeing with earlier observations in ASDEX Upgrade and JET [17]. Comparison of reflectometry data between the HFS and LFS midplane regions in figure 2d suggests that the high-density front extends all the way to the HFS midplane region: beyond the roll-over core density, the SOL density at the HFS midplane increases to 4—8 times higher values than at the LFS midplane. This finding is also consistent with earlier results from ASDEX Upgrade [18].

Divertor plasma oscillations, during which the HFS divertor returns momentarily from almost detached to attached conditions [19,20], were observed within a narrow density region at approximately  $n_e=3.7\times 10^{19} \text{ m}^{-3}$  throughout the discharge 32131. As shown in figures 3a—b, the oscillations appear as periodic increases in the target ion flux and decreases in the HFS divertor volume density and cease momentarily after the neutral beam injection (NBI) blips, used for CXRS measurements at 0.5-s periods, possibly due to a brief increase in the plasma density after each beam blip. The oscillations are also characterized by a 3—6-fold decrease in the HFS SOL midplane density, as suggested by the reflectometry data in figure 3c. The return to attached conditions is evident in figures 3d—e in which both the target ion saturation current and electron temperature are shown to increase by up to an order of magnitude close to the strike point during the oscillations.

#### 4. SOL flows of $\text{N}^+$ ions

The line-integrated SOL flow velocities of injected  $\text{N}^+$  ions were resolved from the Doppler shift of six N(II) lines within 460—465 nm, resulting from the  $2s^22p3p \ ^3P \rightarrow 2s^22p3s \ ^3P$  transition. The radial intensity profiles of the N(II) emission, integrated over the width of the most intense line at 463 nm, are presented in figure 4 in toroidal and poloidal viewing directions. The figure shows that the emission peak shifts away from the separatrix with increasing density due to the collisional nature of ionization and excitation. Thereby, the accuracy of the analysis in the vicinity of the separatrix suffers from low intensities at high densities, and in the subsequent analysis data has been omitted in regions where the intensity of the emission recorded by the signal LOS is less than 50% higher than that of the background LOS. Beyond this point, the fit of the background-corrected spectrum becomes unreliable due to decreased signal-to-noise ratio.

##### 4.1. Measured toroidal and poloidal $\text{N}^+$ flows

At distances larger than 2 cm from the separatrix, co-current flows of approximately 2—10  $\text{kms}^{-1}$  are observed in all densities, increasing with the distance from the separatrix, as shown in figure 5a. Here, the co-current direction corresponds to a parallel flow direction towards the HFS divertor. Closer to the separatrix, the results suggest reversal of the  $\text{N}^+$  flow with velocities up to 7  $\text{kms}^{-1}$  in the counter-current direction for conditions when the HFS divertor is in the high-recycling regime. The region of the reversed flow extends to approximately 2 cm from the separatrix at the lowest densities (32130), while its width is roughly half of this in the medium density cases (32131, 32132). At the highest densities (32133, 32136), when the HFS divertor is in the detached regime, the results do not show reversed flows, and the co-current flow speed is increased by a factor of 2 in comparison to the low-density cases.

In the poloidal direction, the results of the spectroscopic analysis, presented in figure 5b, do not show noticeable differences between the different density cases. For  $R-R_{\text{sep}} < -2$  cm, the poloidal component of the  $N^+$  flow is directed towards the HFS divertor at velocities below  $1 \text{ km s}^{-1}$ . Considering the pitch angle of the magnetic field, this flow magnitude is consistent with the poloidal component of the parallel  $N^+$  flow, when compared to the magnitude of the toroidal component. In the near SOL, the poloidal flow is away from the HFS divertor, increasing up to  $2 \text{ km s}^{-1}$  towards the separatrix. In this region, the direction of the poloidal flow is in contradiction with the toroidal flow component at high densities, hinting at a possible strong contribution of the cross-field  $\mathbf{E}_r \times \mathbf{B}$  drift close to the separatrix. The measured poloidal velocities would correspond to a radial electric field of up to  $7 \text{ kV m}^{-1}$  which is comparable to earlier observations in L-mode plasmas in the LFS SOL of ASDEX Upgrade [21,22]. However, it is noted that the uncertainties of the analysis cause a significant relative error in the poloidal velocities, which complicates both the interpretation of the flow direction and inferring the magnitude of the radial electric field.

The behaviour of the observed  $N^+$  flows with varying density is similar to what was observed for  $C^{2+}$  ions in similar measurements during an L-mode density ramp in [7]. Dominance of the  $\mathbf{E}_r \times \mathbf{B}$  drift in the poloidal near-SOL flow was also suggested by camera imaging of injected nitrogen in Alcator C-Mod [9]. Even though the  $N^+$  ions are not expected to be fully entrained in the  $D^+$  flow, the results are qualitatively consistent with earlier observations of parallel HFS SOL flows of  $D^+$  in ASDEX Upgrade, Alcator C-Mod and JT-60U. In all these devices, the flow speed increases with distance from the separatrix [2,3,5,6]. Reversal of the flow close to the separatrix at low densities was also observed on the HFS midplane of Alcator C-Mod [2] and on the HFS divertor entrance of JT-60U [3]. In JT-60U, detachment of the HFS divertor was found to cancel the reversal in the near SOL and to noticeably increase the flow speed in the far SOL [1], agreeing with the behaviour of the  $N^+$  flows in figure 6a. Increase in flow speed with increasing density was also observed in Alcator C-Mod [2]. On the other hand, the observed increase in  $N^+$  flows at high densities can also be partially due to improved frictional entrainment with the background  $D^+$  flow.

The results of this work together with earlier results of  $D^+$  flows suggest that detachment of the HFS divertor changes the poloidal pressure profile which mostly drives the HFS SOL flow. The reversal of the flow in the near SOL is commonly attributed to ionization of the neutrals recycled from the HFS target in a narrow region close to the separatrix causing the plasma pressure to exceed its upstream value, thus reversing the pressure-driven flow above the ionization region [23]. In the HFS divertor of ASDEX Upgrade, such reversal did not occur [5,6], but the measurements were done below the X point, possibly being already below the strongly localized ionization region. The lack of reversal in detached conditions suggests shifting of the pressure peak from the HFS divertor region to above the HFS midplane.

#### 4.2. Uncertainties of the measurements

The significant uncertainty of the position of the separatrix on the HFS of ASDEX Upgrade was compensated by radial positioning of the  $N^+$  ion temperatures obtained from the Doppler broadening of the spectral lines. Figure 5c shows the radial profiles of the  $N^+$  temperature for each density case measured in both toroidal and poloidal viewing angles. For all densities, the data shows an increase from approximately 20 eV to 60 eV towards the core, but the temperature profile is shifted towards the inner wall with increasing density. Here, it was assumed that the radial position at which the temperature gradient increases towards the core should be roughly the same for all densities, and the aforementioned radial differences are attributed to the uncertainty of the position of the separatrix. Hence, the data have been

shifted by approximately 1 cm towards the core in the high-density cases and by 1 cm away from the core in the low-density cases to obtain the temperature profiles presented in figure 5d. Similar shifts have been applied to the intensity profiles in figure 4 and the flow profiles in figures 5a—b.

With no other measurements of  $T_i$  in the HFS SOL, this assumption can, however, not be fully justified. Equilibration of  $N^+$  and  $D^+$  ions is expected to improve with increasing densities, which could also explain why the steepening of the  $N^+$  temperature profiles occurs further away from the separatrix at high densities in figure 5c. However, the radial shifts mainly affect the width of the region with the reversed flow in high-recycling conditions, having thus only a small effect on the conclusions made from the aforementioned analysis.

Due to uncertainties in wavelength calibration and fitting of the spectral lines, uncertainties of  $\pm 3 \text{ km s}^{-1}$  have been estimated for the flow velocity. For the temperature of the  $N^+$  ions, the uncertainty of the fit corresponds to an error of 5—10 eV, increasing towards the separatrix. An estimated uncertainty of 10% for the instrument broadening of the spectral lines yields an additional error of 10 eV, leading to a total error estimate of 15—20 eV. For clarity, the error bars have been omitted from the figures.

#### 4.3. Effect of divertor plasma oscillations on the $N^+$ flows

The effect of the divertor plasma oscillations, which occurred during the discharge 32131, was observed also in the measured flows. In figure 6a, the toroidal flow velocities measured during and in between the oscillations are presented separately, and a clear division in two branches is observed. During the oscillations, the toroidal flow speed is observed to increase by approximately  $2 \text{ km s}^{-1}$  with the largest effect close to the separatrix, where the direction of the flow changes from reversed to co-current. Figure 6b shows the ion saturation current measured on the HFS target during and in between the oscillations, and the change in the flow direction can be seen to coincide with the region of the most significant increase in the ion saturation current during the oscillations, mapping to within 1 cm of the separatrix at the HFS midplane. Together with the increased target ion flux and decreased HFS SOL density, shown in figures 3a—c, the results suggest increased parallel plasma transport during the oscillations, pushing the high-density front down from the HFS midplane region to the HFS target. The effect is the most dramatic close to the separatrix. The oscillations also shift the peak of the  $N(\text{II})$  intensity profile by approximately 0.5 cm towards the separatrix, as shown in figure 6c, which agrees with the density behaviour of the intensity profiles in figure 4.

### 5. Modelling of the $N^+$ flows

The edge fluid code SOLPS 5.0 was used to predict the SOL conditions in the experiment on a 2-D grid by matching the radial profiles of  $n_e$ ,  $T_{e/i}$  and  $j_{\text{sat}}$  with the diagnostics data as closely as possible in the midplane and target regions. Drift terms were switched on for better representation of the HFS conditions [24,25]. For the time being, a good correspondence has been obtained for  $n_e$  and  $T_{e/i}$  on the LFS midplane and  $n_e$  on the HFS midplane, while the simulations heavily overestimate the measured ion flux on the HFS divertor target by a factor of 10 at high densities after detachment, which may affect the result of the HFS plasma flow due to poorly predicted plasma pressure in the HFS SOL. Thus, the background flow was used as a free parameter in the subsequent modelling. Overestimation of the HFS target flux in SOLPS – especially at high densities – has been reported also earlier in, e.g., [24,26], while more recently progress has been made to overcome the issue by improving the description of the neutral conditions in the HFS divertor with the help of additional convective transport in the LFS SOL [27].

Due to the parametric dependencies of the friction force between the nitrogen impurities and the main plasma ( $F_f \sim Z^2(v_D - v_N)n_i T_i^{-3/2}$ ) [28], the entrainment of the  $N^+$  ions is expected to improve with increasing density. In this work, modelling of the experiment was restricted to discharges 32130 and 32136 to study two extreme cases of the density range.

The SOLPS results on the HFS midplane were extrapolated into background plasmas for the Monte Carlo particle transport code ERO which was used to model the  $N_2$  injection by placing a 3D simulation grid around the point of injection similarly as in [7]. With the help of the emission and velocity output of ERO, it is possible to mimic the line-integrated Doppler spectroscopy measurements along the same lines-of-sight as in the experiment, as described in [29].

The shape and magnitude of the radial profile of the background plasma flow was varied until the line-integrated  $N^+$  flow agreed with the measured profiles. Additionally, the plasma temperature at the HFS midplane had to be scaled down by 25% in the high-density case and by up to 90% in the low-density case to reproduce the measured  $N^+$  flow profiles via improved frictional entrainment. Since the injected  $N_2$  does not affect the fixed background plasma in ERO simulations, the downscaling of the temperature can partially be attributed to the expected local cooling of the plasma due to interactions between the neutral nitrogen molecules and atoms and the background plasma close to the injection point. However, since the radiative cooling is expected to be stronger at high densities, this may also point out that the initial low-density SOLPS solutions were overestimating the  $D^+$  ion temperature for which there was no experimental data in the SOL.

The radial profiles of the HFS plasma parameters used in the ERO modelling and the resulting toroidal and poloidal  $N^+$  flows are presented in figure 7 for the cases with the best match between measured and simulated  $N^+$  flows at the highest and lowest densities. The results show entrainment of 20—40% at high density and 10—20% at low density between the toroidal  $N^+$  and  $D^+$  flow magnitudes. The shapes of the  $N^+$  and  $D^+$  flow profiles are roughly similar with lower entrainment towards the inner wall, where the plasma density is decreased. In the low-density case, the region of reversed flow is approximately 1 cm narrower for  $D^+$  than for  $N^+$ , which is an effect of line-integration of the  $N^+$  velocity in the curved plasma. In the poloidal direction, radial electric fields of approximately  $3 \text{ kV m}^{-1}$  and  $7 \text{ kV m}^{-1}$  were required in the low- and high-density cases, respectively, to reproduce the measured velocities in the near SOL, supporting the experimental hypothesis made in section 4.1. Overall, the results suggest that the line-integrated measurements with  $N^+$  ions are qualitatively indicative for the  $D^+$  flows, while the quantitative consistency could be improved by, e.g., considering  $N^{2+}$  or  $N^{3+}$  ions for which ERO predicted 2—3 times better frictional entrainment than for  $N^+$ .

## 6. Conclusions

Flows of injected  $N^+$  ions were measured in the SOL at the HFS midplane of ASDEX Upgrade by Doppler spectroscopy with different degrees of HFS divertor detachment. The results show reversal of the  $N^+$  flow close to the separatrix in high-recycling conditions and flow towards the HFS divertor in the detached regime, suggesting shifting of the peak of the poloidal pressure profile from the HFS divertor to above the HFS midplane in detachment. In addition, divertor plasma oscillations at intermediate upstream densities were found to momentarily increase the plasma flow towards the HFS divertor, overcoming the reversal and pushing the high-density front back from the HFS midplane to the HFS target.

ERO simulations of the  $N_2$  injection in the highest- and lowest-density cases of the experiment showed entrainment ratios below 40% and 20%, respectively, between the flow velocities of  $N^+$  and  $D^+$ . The results thus suggest that  $N^+$  gives a qualitative indication of the  $D^+$  flow but is quantitatively not suitable as a proxy for measuring its magnitude. To study the prospects of improved entrainment of higher charge states, new measurements have been performed with similar plasmas by recording the emission of  $N^{2+}$  ions. The analysis of this experiment will be reported elsewhere.

## Acknowledgments

This work has been carried out within the framework of the EUROfusion Consortium and has received funding from the Euratom research and training programme 2014-2018 under grant agreement number 633053 [and from Tekes – the Finnish Funding Agency for Innovation under the FinnFusion Consortium]. The views and opinions expressed herein do not necessarily reflect those of the European Commission.

Work performed under EUROfusion WP PFC.

## References

- [1] N. Asakura, *Journal of Nuclear Materials* **363—365** (2007) 51—51
- [2] B. LaBombard et al., *Nuclear Fusion* **44** (2004) 1047—1066
- [3] N. Asakura et al., *Nuclear Fusion* **44** (2004) 503—512
- [4] N. Smick et al., *Nuclear Fusion* **53** (2013) 023001
- [5] H.W. Müller et al., *Journal of Nuclear Materials* **363—365** (2007) 605—610
- [6] M. Tsalas et al., *Plasma Physics and Controlled Fusion* **49** (2007) 857—872
- [7] T. Makkonen et al., *Journal of Nuclear Materials* **438** (2013) S410—S413
- [8] J. Karhunen et al., *Proceedings of Science (ECPD 2015)* 038
- [9] B. LaBombard et al., *22<sup>nd</sup> International Conference on Plasma Surface Interactions in Controlled Fusion Devices* (2016) I19
- [10] R. Schneider et al., *Contributions to Plasma Physics* **46** (2006) 3—191
- [11] A. Kirschner et al., *Nuclear Fusion* **40** (2000) 989
- [12] M. Weinlich et al., *Contributions to Plasma Physics* **36** (1996) 53—60
- [13] S. Potzel et al., *Plasma Physics and Controlled Fusion* **56** (2014) 025010
- [14] A. Silva et al., *Review of Scientific Instruments* **70** (1999) 1072—1075
- [15] T. Pütterich et al., *Nuclear Fusion* **52** (2012) 083013
- [16] E. Viezzer et al., *Plasma Physics and Controlled Fusion* **55** (2013) 124037
- [17] S. Potzel et al., *Journal of Nuclear Materials* **463** (2015) 541—545
- [18] L. Guimarais et al., *42<sup>nd</sup> EPS Conference on Plasma Physics* (2015) P1.111

- [19] S. Potzel et al., *Journal of Nuclear Materials* **438** (2013) S285—S290
- [20] A. Loarte et al., *Physical Review Letters* **83** (1999) 3657—3660
- [21] H.W. Müller et al., *Nuclear Fusion* **51** (2011) 073024
- [22] G.D. Conway et al., *Plasma Physics and Controlled Fusion* **57** (2015) 014035
- [23] S.I. Krasheninnikov, *Nuclear Fusion* **32** (1992) 1927—1934
- [24] M. Wischmeier et al., *Journal of Nuclear Materials* **390—391** (2009) 250—254
- [25] L. Aho-Mantila et al., 41<sup>st</sup> EPS Conference on Plasma Physics (2014) O4.120
- [26] L. Aho-Mantila et al., *Nuclear Fusion* **52** (2012) 103006
- [27] F. Reimold et al., 22<sup>nd</sup> International Conference on Plasma Surface Interactions in Controlled Fusion Devices (2016) O15
- [28] J. Neuhauser et al., *Nuclear Fusion* **24** (1984) 39—47
- [29] T. Makkonen et al., *Computer Physics Communications* **184** (2013) 1842—1847

## Figure captions

**Figure 1:** Time traces of line-integrated core electron density during the discharges used in the experiment.

**Figure 2:** Integrated total ion flux (a) and strike-point electron temperature (b) on the HFS divertor target as a function of the core electron density during the different discharges. Evolution and propagation of the HFS high-density front vertically in the divertor volume (c). The coordinate  $\Delta S$  increases upwards from the strike point ( $\Delta S=0$ ) along the target plate, and the white dashed line marks the roll-over density. Comparison of the HFS and LFS reflectometry data (d) shows an increase in the HFS SOL density also in the midplane region.

**Figure 3:** During the discharge 32131, the divertor plasma oscillations appear as periodic peaks in the time trace of the HFS target ion flux (a) and decreases in the divertor density (b). The coordinate  $\Delta S$  is defined as in figure 2c. On the HFS midplane, the oscillations are connected to a decrease in the electron density (c). Return to attached conditions is seen as significant increases in the ion saturation current (d) and electron temperature (e) on the HFS target.

**Figure 4:** The radial profiles of the N(II) emission intensity recorded in toroidal (a) and poloidal (b) angles during a radial plasma sweep.

**Figure 5:** The measured radial velocity profiles of toroidal (a) and poloidal (b)  $N^+$  flows. The measured radial  $N^+$  temperature profiles before (c) and after (d) shifting the data radially for consistency.

**Figure 6:** The radial profiles of toroidal  $N^+$  flows (a) and ion saturation current on the HFS target (b) during and in between the divertor plasma oscillations for the discharge 32131. The  $R-R_{sep}$  axis in (b) has been mapped to 13 cm above the HFS midplane for comparability. The radial intensity profiles (c) of N(II) emission during and in between the oscillations.

**Figure 7:** Radial profiles of  $n_e$  (a),  $T_{e/i}$  (b) and  $v_{D^+,||}$  (c) on the HFS midplane in the ERO simulations providing the best match with the measured  $N^+$  velocities in toroidal (d) and poloidal (e) directions for the highest- and lowest-density cases.

## Figures

### Figure 1

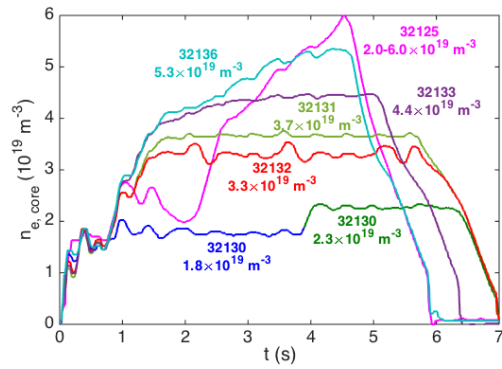


### Figure 2

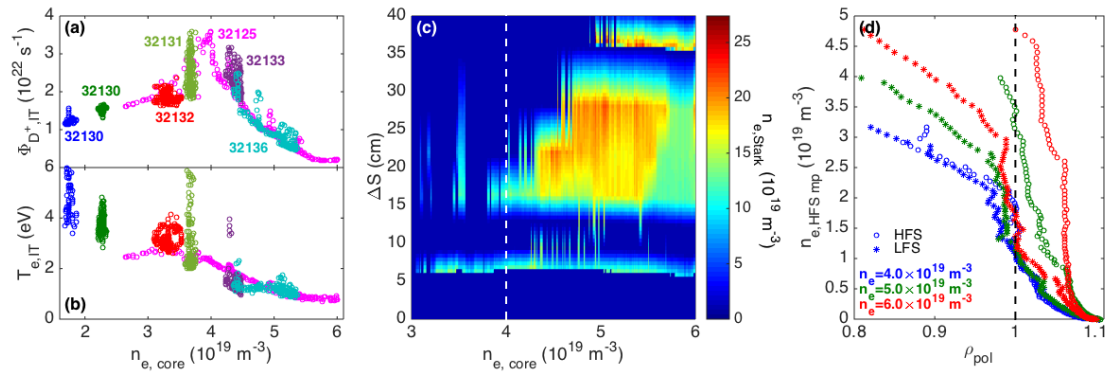


### Figure 3

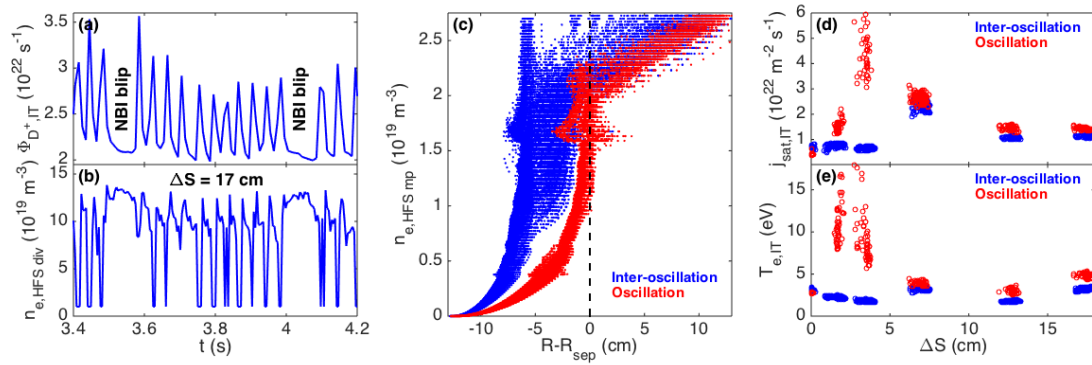


**Figure 4**

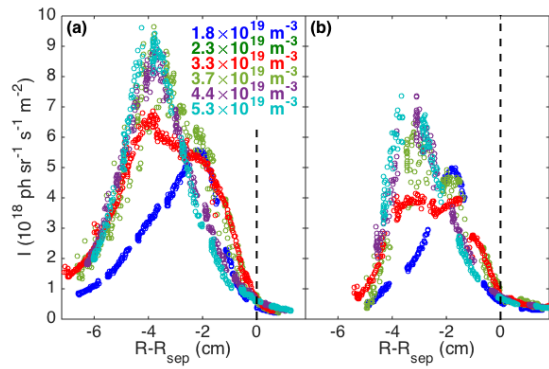


**Figure 5**

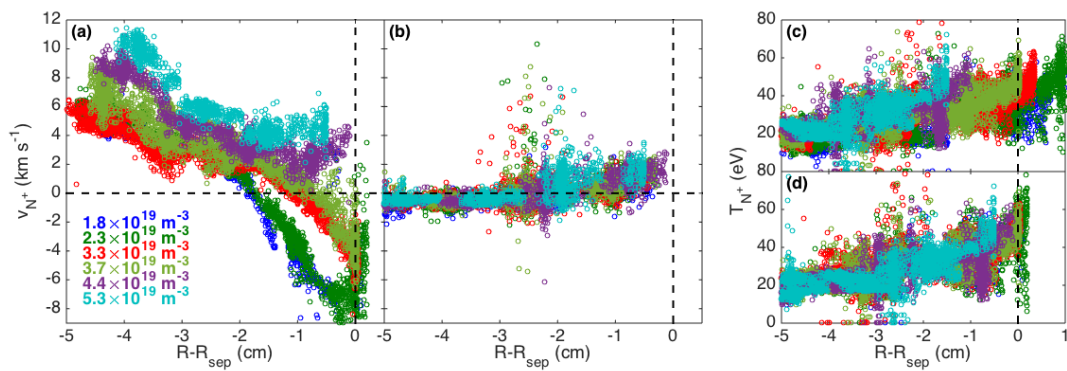


**Figure 6**

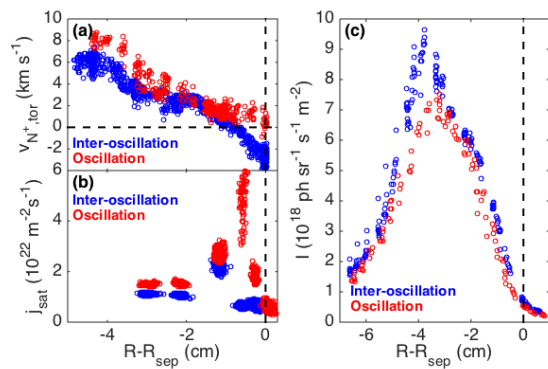


**Figure 7**

